Unsolvated 5,10,15,20-tetra-4-pyridyl-porphyrin, its sesquihydrate and its 2-chlorophenol disolvate: conformational versatility of the ligand

Sophia Lipstman and Israel Goldberg*

School of Chemistry, Sackler Faculty of Exact Sciences, Tel-Aviv University, Ramat-Aviv, 69978 Tel-Aviv, Israel
Correspondence e-mail: goldberg@post.tau.ac.il

Unsolvated 5,10,15,20-tetra-4-pyridylporphyrin, $C_{40}H_{26}N_8$, (I), its sesquihydrate, $C_{40}H_{26}N_8 \cdot 1.514H_2O$, (II), and its 2-chlorophenol disolvate, $C_{40}H_{26}N_8 \cdot 2C_6H_5ClO$, (III), reveal different conformational features of the porphyrin core. In (I), the latter is severely deformed from planarity, apparently in order to optimize the intermolecular interactions and efficient crystal packing of the molecular entities. The molecular framework has a C_1 symmetry. In (II), the porphyrin molecules are located on $\bar{4}$ symmetry axes, preserving the marked deformation from planarity of the porphyrin core. The molecular units are interlinked into a single-framework supramolecular architecture by hydrogen bonding to one another *via* molecules of water, which lie on twofold rotation axes. In (III), the porphyrin molecules are located across centres of inversion and are characterized by a planar conformation of the 24-membered macrocyclic porphyrin ring. Two *trans*-related pyridyl substituents are hydrogen bonded to the 2-chlorophenol solvent molecules. The interporphyrin organization in (III) is similar to that observed for many other tetraarylporphyrin compounds. However, the organization observed in (I) and (II) is different and of a type rarely observed before. This study reports for the first time the crystal structure of the unsolvated tetrapyridylporphyrin.

Comment

Tetrapyridylporphyrin (TPyP; Fleischer, 1962), (I), is one of the most widely studied porphyrin ligands in materials chemistry. It bears laterally diverging pyridyl functions, which can readily interact in a co-operative manner with complementary entities through either coordination or hydrogen bonding. Moreover, it can form organometallic complexes with various transition metal ions inserted into the macrocyclic core, the latter potentially providing additional binding sites for further intermolecular coordination. Self-coordination of the Zn–TPyP complex into one-, two- and three-dimensional

coordination polymers has been widely reported (Fleischer & Shachter, 1991; Krupitsky *et al.*, 1994; Diskin-Posner *et al.*, 2001; Ring *et al.*, 2005). Facile formation of diverse coordination networks and frameworks of TPyP and *M*–TPyP *via* metal ions as bridging nodes between the peripheral pyridyl functions of adjacent species has also been reported (Goldberg, 2000, 2005, 2008, and references therein). More recently, the capacity of this porphyrin to engage in networking by supramolecular hydrogen bonding through complementary components has been demonstrated (Koner & Goldberg, 2009). The molecular framework of TPyP/Zn–TPyP is relatively rigid, and the central core of the porphyrin has an aromatic nature. However, the detailed conformation of this ligand is affected to some extent by the requirement to optimize the intermolecular interactions, and minimize the enthalpy, within the formed supramolecular assembly in a given case. Correspondingly, the macrocyclic framework of TPyP may reveal in most cases either flat or slightly ruffled conformations, as has been observed for various tetrapyrrole macrocycles (Scheidt & Lee, 1987). Like many other tetra-arylporphyrins, the TPyP/*M*–TPyP framework exhibits shape complementarity only in two dimensions (Byrn *et al.*, 1993, and references therein), and therefore it commonly tends to crystallize as a solvate (because of this feature such compounds were nicknamed 'porphyrin sponges'), where molecules of the solvent fill the interporphyrin voids in the lattice. This may explain why the crystal structure of unsolvated TPyP has not been characterized previously.
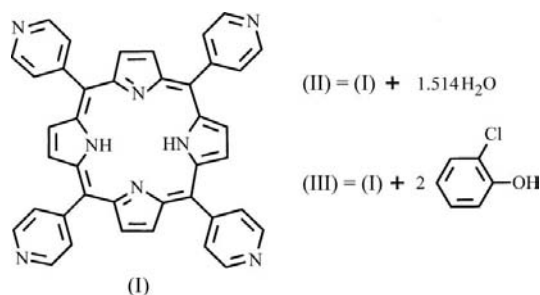
We report here for the first time the crystal structure of pure TPyP, (I), and relate it to the unique conformational features of the porphyrin ligand in this case. We also describe the structure of the sesquihydrate TPyP·1.514H_2O, (II), in which an unusually large deformation of the porphyrin core has again been observed, apparently also in order to facilitate multiple supramolecular hydrogen bonds between the porphyrin and water components. Then, another variant, 2-chlorophenol solvated TPyP, (III), is described, in which, however, the porphyrin macrocycle is characterized by a nearly planar conformation. The molecular structure of (I) is shown in Figs. 1 and 2(*a*). Of particular interest is the severe deformation of the porphyrin core from planarity, resulting from the optimization of the intermolecular packing in the crystals of pure TPyP. Fig. 2(*a*) gives the deviations of the individual atoms from the mean plane of the 24-membered porphyrin core, which range from −0.394 (for atom C7) to

organic compounds
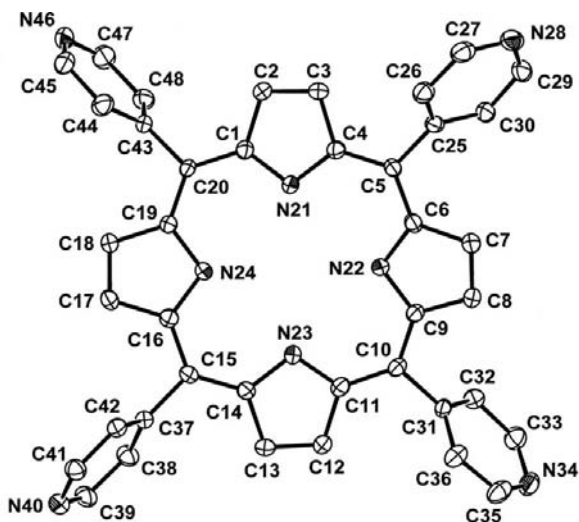
Figure 1
The molecular structure of (I), showing the atom-labelling scheme. The atom ellipsoids represent displacement parameters at the 50% probability level at *ca* 110 K. H atoms have been omitted.
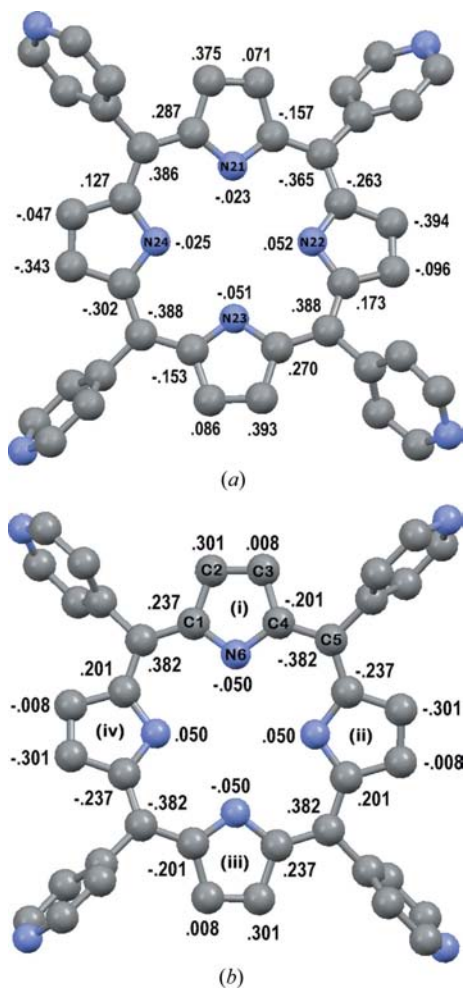
Figure 2
Deviations of the individual atoms (Å) from the mean plane of the 24-membered porphyrin core in (*a*) (I) and (*b*) (II), indicative of similar severe ruffling of the macrocycle in the two compounds. [Symmetry codes: (i) *x, y, z*; (ii) −*y, x*, −*z* + 1; (iii) −*x*, −*y, z*; (iv) *y*, −*x*, −*z* + 1.]

0.393 Å (C12). The relatively large dihedral angles between the planes of the five-membered pyrrole rings provide further evidence for the severe ruffling of this porphyrin macrocycle. Thus, the dihedral angles between the corresponding adjacent pyrrole rings (those containing atoms N22/N21, N23/N22, N24/N23 and N21/N24) are 18.19 (6), 20.20 (10), 20.34 (11) and 17.25 (9)°, respectively. The dihedral angles between pyrrole rings located across the macrocycle are even larger [27.44 (9)° for N23/N21 and 26.41 (8)° for N24/N22]. The molecular symmetry of TPyP in this structure is C_1. The conformationally distorted porphyrin molecules pack tightly in the crystal structure of (I), without the need to incorporate crystallization solvent into the lattice, as shown in Fig. 3. The intermolecular organization is stabilized effectively by van der Waals forces. The porphyrin core of a given molecule is approached from above and below by edge-on-oriented pyridyl substituents of neighbouring species. Nearly parallel overlap between the pyridyl rings of the laterally displaced units is indicative of possible π–π interactions between them. However, no direction-specific intermolecular contacts, such as those of C—H⋯N type, significantly shorter than the corresponding sums of the van der Waals radii are present.

The porphyrin molecule in (II) is also characterized by a distorted conformation of the central core (Figs. 2*b* and 4). In this structure the porphyrin molecular unit is located on the $\overline{4}$ axis of symmetry, while the water species reside on twofold axes. The dihedral angles between the adjacent pyrrole rings are 18.27 (8)°; those between the pyrroles across the macrocycle are 25.95 (7)°. The deviations of the individual atoms in the 24-membered macrocycle are quite significant, as in (I), ranging from −0.382 to 0.382 Å (Fig. 2*b*). Water molecules located on twofold rotation axes, and with site occupancy 0.757 (10), form hydrogen bonds to the peripheral pyridyl N atoms of two adjacent porphyrin units located at different *z*-coordinate levels (Fig. 5 and Table 1). These interactions operate at the four corners of the ligand, throughout the crystal, thus creating a continuous three-dimensional hydrogen-bonded architecture. Fig. 6 illustrates the crystal
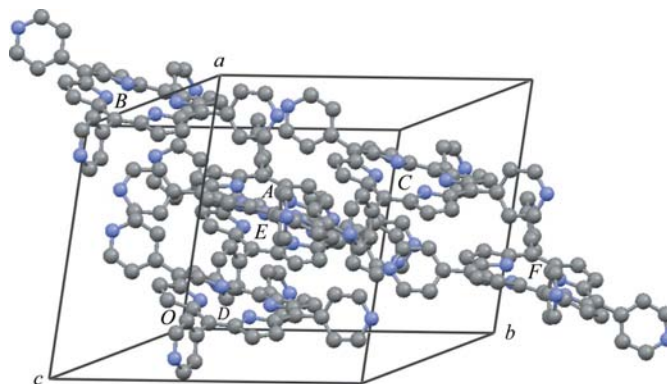
Figure 3
The crystal packing of (I). Note that the porphyrin core of porphyrin *A* is approached from above and below by nearly parallel pairs of the pyridyl arms of molecules *B* and *C* (above), and *D* and *E* (below). [Symmetry codes: (*A*) $x + \frac{1}{2}$, $-y + \frac{1}{2}$, $z + \frac{1}{2}$; (*B*) $x + 1$, y, $z + 1$; (*C*) $x + \frac{1}{2}$, $y + \frac{1}{2}$, z; (*D*) x, y, z; (*E*) $x + \frac{1}{2}$, $y + \frac{1}{2}$, $z + 1$; (*F*) x, $-y + 1$, $z - \frac{1}{2}$.]

packing of (II) viewed roughly perpendicular to the tetragonal axis, depicting the distorted nature of the porphyrin macrocycle. The TPyP molecules are arranged along the c axis in an offset manner, so that the macrocycle of a given unit is approached from a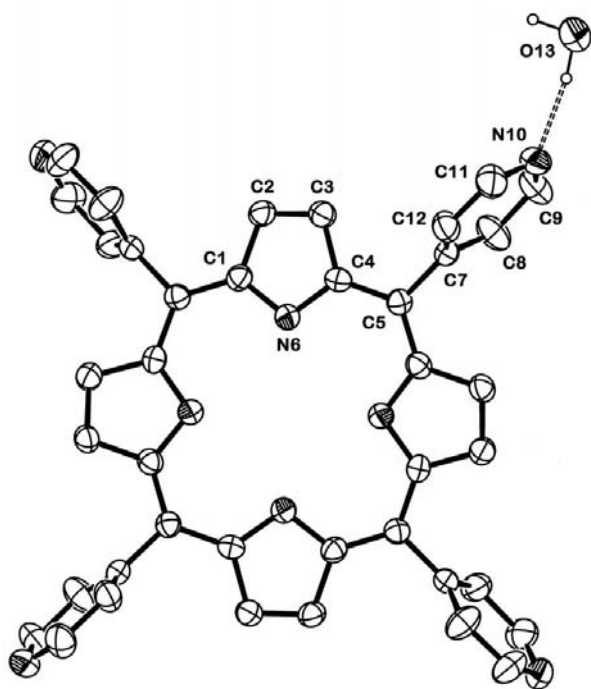bove and below by two pyridyl groups of adjacent porphyrins on each side. The tight arrangement lacks intermolecular contacts that are significantly shorter than common van der Waals diameters, reflecting on further (to the hydrogen-bonding interactions) stabilization of the entire structure by common dispersion forces.

While TPyP reveals similarly distorted conformations in the two previous examples, this is not the case in the structure of its 2-chlorophenol disolvate (III) (Fig. 7). The porphyrin molecule is located across the inversion centre at $(\frac{1}{2}, \frac{1}{2}, \frac{1}{2})$, and its two *trans*-related pyridyl groups are hydrogen bonded to the 2-chlorophenol solvent. The macrocyclic core is essentially planar, and the TPyP molecules are stacked in an offset manner along the a axis of the crystal at a mean interplanar distance of 3.55 (2) Å (Fig. 8). In this offset stacked geometry, each porphyrin core is sandwiched between two pyridyl arms

Figure 4
The molecular structure of (II), showing the atom-labelling scheme. The porphyrin molecules are located on $\bar{4}$ symmetry axes, and only atoms of the asymmetric unit are labelled. The atom ellipsoids represent displacement parameters at the 50% probability level at *ca* 110 K. All H atoms except those of the water molecule have been omitted. The hydrogen bonding of the water molecule to the pyridyl group is denoted by dashed lines.
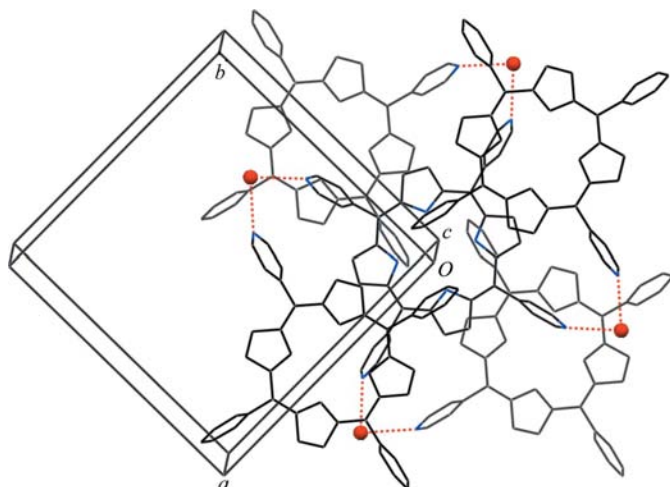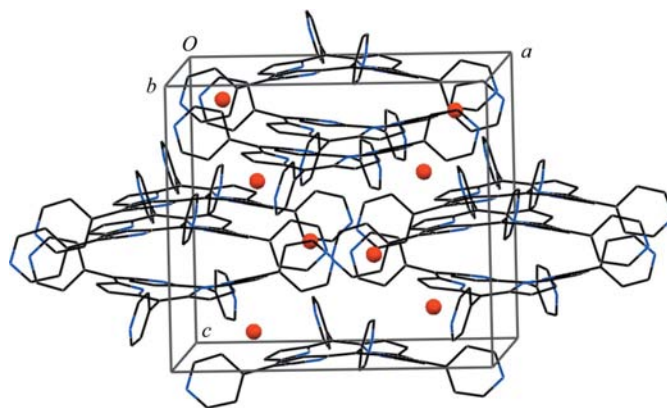

Figure 6
A wireframe illustration of the crystal structure of (II). The water molecules are depicted as small spheres and all H atoms have been omitted.

Figure 5
The hydrogen-bonding interactions in (II), indicated by dashed lines. The water molecules are depicted as small spheres and all H atoms have been omitted. The viewing perspective is nearly down the tetragonal axis. Note that the central porphyrin molecule is hydrogen bonded to four other porphyrin units located at either higher or lower z-coordinate levels of the structure.
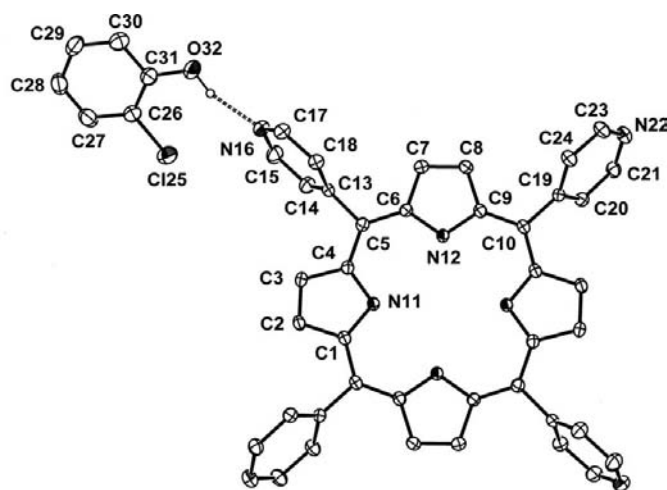

Figure 7
The molecular structure of (III), showing the atom-labelling scheme. The porphyrin molecules are located on inversion centres, and only atoms of the asymmetric unit are labelled. The atom ellipsoids represent displacement parameters at the 50% probability level at *ca* 110 K. All H atoms except those of the hydroxy group have been omitted. The hydrogen bonding of the 2-chlorophenol molecule to the pyridyl group is denoted by a dashed line.

organic compounds

of adjacent species from above and below, which are displaced by $\pm b$. Porphyrin stacks displaced along the c axis form tightly packed layered zones parallel to the ac face of the unit cell. Within this zone, the *trans*-related pyridyl groups of neighbouring coplanar porphyrins overlap effectively, stabilizing the layered arrangement by favourable dipolar and dispersive interactions. The other pyridyl substituents, directed outwards (perpendicular to the layered porphyrin arrays), are hydrogen bonded to the 2-chlorophenol species *via* O—H···N hydrogen bonds (Table 2). This intermolecular organization is similar to that reported for the 1:2 TPyP solvates with guaiacol and benzyl alcohol (Krupitsky *et al.*, 1994), and is frequently found in solvates of other tetraarylporphyrins (Byrn *et al.*, 1993, and references therein). The interporphyrin offset stacking geometry is a fundamental property of the porphyrin–porphyrin interaction (Leighton *et al.*, 1988), and structure (III) is in agreement with this principle. In crystals, it favours stacked organization of the tetraarylporphyrin molecules with flat cores, and tight packing of these stacks into two-dimensional layers. The crystalline organization of the two-dimensional porphyrin layers along the third dimension is facilitated by solvation of the layers along the interfaces between them.

This study characterizes for the first time the structure of unsolvated TPyP, revealing an unusually distorted conformation of this ligand. This observation is even more striking when compared with the structure of the solvent-free tetraphenylporphyrin analog (TPP), which reveals a planar conformation of the porphyrin core and the common offset stacking arrangement as in (III) (Kano *et al.*, 2000). It is possible that the electron-withdrawing effect of the pyridyl substituents weakens the aromaticity of the porphyrin macrocycle in TPyP (as compared with that in TPP), allowing more readily its deformation from planarity by more dominant crystal packing forces. It appears that this feature is conserved even in the presence of small solvent molecules such as water [as in (II)], while with larger solvent molecules, such as 2-chlorophenol [as in (III)], the more abundant offset stacked organization of TPyP is formed. It remains to be seen whether a flat polymorph of unsolvated TPyP will be found in the future.

Figure 8
(*a*) The crystal structure of (III), showing nine parallel stacks of TPyP molecules displaced by $\pm b$ and $\pm c$, and interspaced by the 2-chlorophenol solvent molecules. (*b*) A parallel view of the overlapping mode between neighbouring porphyrin species in the stack [at (x, y, z) and $(x \pm 1, y, z)$]. Note the offset of the molecular frameworks, which allows the pyridyl group of one unit to perch over the porphyrin centre of an adjacent unit. The mean distance between the overlapping 11-atom fragments of the relevant porphyrin rings is 3.55 (4) Å. [Symmetry codes: (i) x, y, z; (ii) $-x + 1, -y + 1, -z + 1$; (iii) $x - 1, y, z$; (iv) $-x, -y + 1, -z + 1$.]

Experimental

The porphyrin compound, as well as all the other reactants and solvents (see below), were obtained commercially. Crystals of (I) and (II) were obtained as by-products during attempts to synthesize coordination networks of the porphyrin moiety with lanthanide ions. Crystals of (I) were obtained by slow diffusion between layers: TPyP (0.011 mmol) was dissolved in a methanol–tetrachloroethane mixture (2 ml, 1:1 *v*/*v*), which was heated under reflux for 2 h and then filtered. A solution of lanthanum chloride heptahydrate (0.9 mmol) in a mixture of methanol and dimethylformamide (5 ml, 5:3 *v*/*v*) was carefully layered on top of the TPyP solution. Crystals were obtained in the porphyrin phase after 12 d. Compound (I) was obtained also in a similar experiment while using gadolinium nitrate hexahydrate instead of the lanthanum salt. For (II), TPyP (0.013 mmol) and lanthanum nitrate hexahydrate (0.092 mmol) were dissolved in a mixture of methanol and 1,2-dichlorobenzene (15 ml, 1:1 *v*/*v*). The resulting solution was heated under reflux and filtered, and the solute was kept for crystallization by slow evaporation. X-ray quality crystals were obtained after one month. In the third case, an attempt to synthesize hydrogen-bonding supramolecular networks by reacting TPyP with thiophene-2,5-dicarboxylic acid (TPDA) failed, yielding instead compound (III). TPyP (0.006 mmol) and TPDA (0.02 mmol) were dissolved in 5 ml of methanol containing a few drops of 2-chlorophenol. The resulting solution was heated under reflux for 10 min and then filtered. Using the slow vapour diffusion method, an open vial of the solute was placed in a closed vessel with diethyl ether. Crystals of (III) appeared after one day.
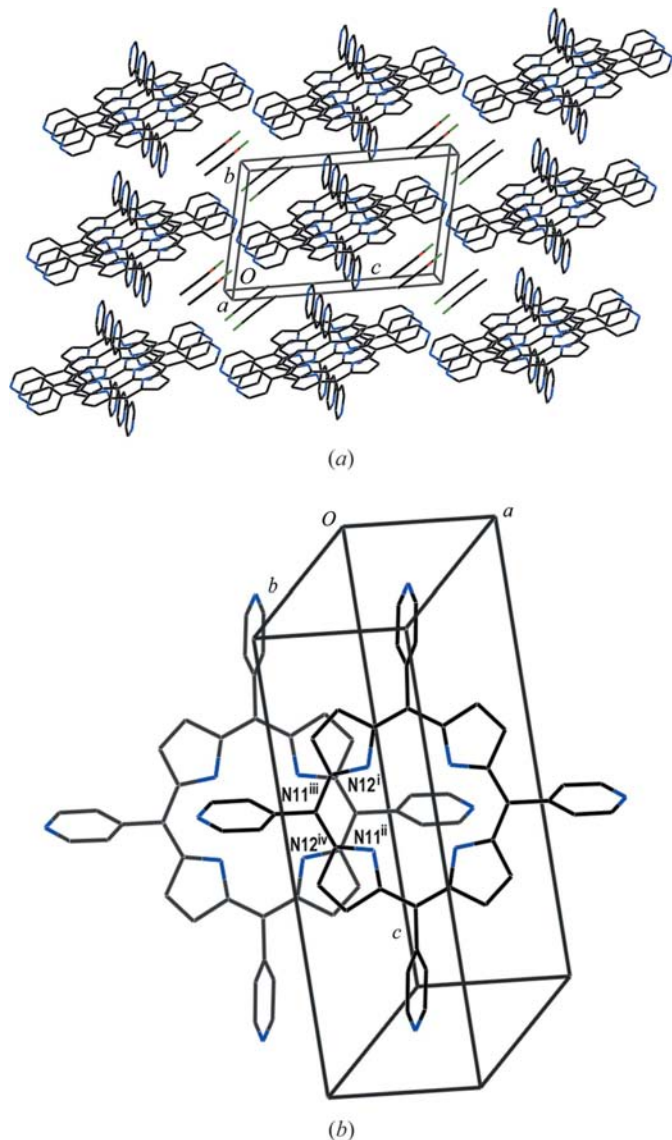
Compound (I)

Crystal data

$C_{40}H_{26}N_8$
$M_r = 618.69$
Monoclinic, Cc
$a = 13.6042 (2)$ Å
$b = 20.8734 (4)$ Å
$c = 11.4525 (2)$ Å
$\beta = 116.2786 (11)°$

$V = 2916.02 (9)$ Å^3
$Z = 4$
Mo $K\alpha$ radiation
$\mu = 0.09$ mm^{-1}
$T = 110$ K
$0.40 \times 0.40 \times 0.30$ mm

Data collection

Nonius KappaCCD diffractometer
16180 measured reflections
3456 independent reflections

3032 reflections with $I > 2\sigma(I)$
$R_{int} = 0.057$

Refinement

$R[F^2 > 2\sigma(F^2)] = 0.049$
$wR(F^2) = 0.127$
$S = 1.06$
3456 reflections
433 parameters

2 restraints
H-atom parameters constrained
$\Delta\rho_{max} = 0.38$ e Å^{-3}
$\Delta\rho_{min} = -0.28$ e Å^{-3}

Compound (II)

Crystal data

$C_{40}H_{26}N_8 \cdot 1.514H_2O$
$M_r = 645.96$
Tetragonal, $I\bar{4}2d$
$a = 15.2155 (4)$ Å
$c = 13.5388 (6)$ Å
$V = 3134.39 (18)$ Å^3

$Z = 4$
Mo $K\alpha$ radiation
$\mu = 0.09$ mm^{-1}
$T = 110$ K
$0.35 \times 0.25 \times 0.15$ mm

Data collection

Nonius KappaCCD diffractometer
16180 measured reflections
1042 independent reflections

757 reflections with $I > 2\sigma(I)$
$R_{int} = 0.067$

Refinement

$R[F^2 > 2\sigma(F^2)] = 0.051$
$wR(F^2) = 0.115$
$S = 1.04$
757 reflections
118 parameters
1 restraint

H atoms treated by a mixture of
independent and constrained
refinement
$\Delta\rho_{max} = 0.13$ e Å^{-3}
$\Delta\rho_{min} = -0.16$ e Å^{-3}

Table 1
Hydrogen-bond geometry (Å, °) for (II).

$D-H\cdots A$	$D-H$	$H\cdots A$	$D\cdots A$	$D-H\cdots A$
O13—H13⋯N10	0.95 (2)	1.902 (13)	2.823 (3)	163 (4)

Compound (III)

Crystal data

$C_{40}H_{26}N_8 \cdot 2C_6H_5ClO$
$M_r = 875.79$
Triclinic, $P\bar{1}$
$a = 6.5563 (2)$ Å
$b = 10.0441 (3)$ Å
$c = 16.1903 (5)$ Å
$\alpha = 77.841 (2)°$
$\beta = 88.9097 (19)°$

$\gamma = 79.6939 (14)°$
$V = 1025.24 (5)$ Å^3
$Z = 1$
Mo $K\alpha$ radiation
$\mu = 0.21$ mm^{-1}
$T = 110$ K
$0.60 \times 0.20 \times 0.10$ mm

Data collection

Nonius KappaCCD diffractometer
11144 measured reflections
4834 independent reflections

3617 reflections with $I > 2\sigma(I)$
$R_{int} = 0.036$

Refinement

$R[F^2 > 2\sigma(F^2)] = 0.058$
$wR(F^2) = 0.156$
$S = 1.03$
4834 reflections

289 parameters
H-atom parameters constrained
$\Delta\rho_{max} = 0.42$ e Å^{-3}
$\Delta\rho_{min} = -0.70$ e Å^{-3}

Table 2
Hydrogen-bond geometry (Å, °) for (III).

$D-H\cdots A$	$D-H$	$H\cdots A$	$D\cdots A$	$D-H\cdots A$
O32—H32⋯N16	0.93	1.90	2.764 (3)	154

In all three compounds, H atoms bound to C atoms were located in calculated positions and were constrained to ride on their parent atoms, with C—H distances of 0.95 Å and $U_{iso}(H)$ values of $1.2U_{eq}(C)$. The two pyrrole N-bound H atoms were found to be disordered between the four pyrrole sites. They were also located in calculated positions and constrained to ride on their parent atoms, with N—H distances of 0.88 Å and $U_{iso}(H)$ values of $1.2U_{eq}(N)$. The H atom bound to O32 in (III) was located in a difference Fourier map, but its position was not refined. The water H atom in the asymmetric unit of (II) could not be located reliably, as the residual electron-density peaks that could correspond to this H atom were very low. One of these peaks was assigned as the H atom, and its position was restrained in the refinement at an O—H distance of 0.95 (2) Å. These H atoms were assigned $U_{iso}(H)$ values of 1.5 and 1.2 times $U_{eq}(O)$ in (II) and (III), respectively. The refined site occupancy of the water molecule in (II) was 0.757 (10) for the crystal selected for data collection, which corresponds to the sesquihydrate with a 1:1.5 porphyrin–water stoichiometry. 14 reflections in (I) and 1 reflection in (II) were omitted from the final structure-factor calculations because of poor assessment of the intensities (oversaturated or overlapping reflections).

For all compounds, data collection: *COLLECT* (Nonius, 1999); cell refinement: *DENZO* (Otwinowski & Minor, 1997); data reduction: *DENZO*; program(s) used to solve structure: *SIR97* (Altomare *et al.*, 1999); program(s) used to refine structure: *SHELXL97* (Sheldrick, 2008); molecular graphics: *ORTEPIII* (Burnett & Johnson, 1996) and *Mercury* (Macrae *et al.*, 2006); software used to prepare material for publication: *SHELXL97*.

References

Altomare, A., Burla, M. C., Camalli, M., Cascarano, G. L., Giacovazzo, C., Guagliardi, A., Moliterni, A. G. G., Polidori, G. & Spagna, R. (1999). *J. Appl. Cryst.* **32**, 115–119.
Burnett, M. N. & Johnson, C. K. (1996). *ORTEPIII*. Report ORNL-6895. Oak Ridge National Laboratory, Tennessee, USA.
Byrn, M. P., Curtis, C. J., Hsiou, Y., Khan, S. I., Sawin, P. A., Tendick, S. K., Terzis, A. & Strouse, C. E. (1993). *J. Am. Chem. Soc.* **115**, 9480–9497.

organic compounds

Diskin-Posner, Y., Patra, G. K. & Goldberg, I. (2001). *J. Chem. Soc. Dalton Trans.* pp. 2775–2782.

Fleischer, E. B. (1962). *Inorg. Chem.* **1**, 493–495.

Fleischer, E. B. & Shachter, A. M. (1991). *Inorg. Chem.* **30**, 3763–3769.

Goldberg, I. (2000). *Chem Eur. J.* **6**, 3863–3870.

Goldberg, I. (2005). *Chem. Commun.* pp. 1243–1254.

Goldberg, I. (2008). *CrystEngComm*, **10**, 637–645.

Kano, K., Fukuda, K., Wakami, H., Nishiyobu, R. & Pasternack, R. F. (2000). *J. Am. Chem. Soc.* **122**, 7494–7502.

Koner, R. & Goldberg, I. (2009). *CrystEngComm*, **11**, 1217–1219.

Krupitsky, H., Stein, Z., Goldberg, I. & Strouse, C. E. (1994). *J. Inclusion Phenom. Mol. Recognit. Chem.* **30**, 177–192.

Leighton, P., Cowan, J. A., Abraham, R. J. & Sanders, J. K. M. (1988). *J. Org. Chem.* **53**, 733–740.

Macrae, C. F., Edgington, P. R., McCabe, P., Pidcock, E., Shields, G. P., Taylor, R., Towler, M. & van de Streek, J. (2006). *J. Appl. Cryst.* **39**, 453–457.

Nonius (1999). *COLLECT*. Nonius BV, Delft, The Netherlands.

Otwinowski, Z. & Minor, W. (1997). *Methods in Enzymology*, Vol. 276, *Macromolecular Crystallography*, Part A, edited by C. W. Carter Jr & R. M. Sweet, pp. 307–326. New York: Academic Press.

Ring, D. J., Aragoni, M. C., Champness, N. R. & Wilson, C. (2005). *CrystEngComm*, **7**, 621–623.

Scheidt, W. R. & Lee, Y. J. (1987). *Struct. Bond.* **64**, 1–71.

Sheldrick, G. M. (2008). *Acta Cryst.* A**64**, 112–122.